

CHAPTER 4

Results and discussion

4.1 Collection and extraction of plant materials

The leaves of *D. obtusipetalum* were collected at Doi-Tung, Chiang Rai Province, Thailand in June 2011. The dried leaves were extracted with 95 % ethanol at room temperature for 3 days and 3 times. The extracts were evaporated using a rotary evaporator to obtain 430 g of dark brown gum crude extract.

4.2 Alkaloids extraction and isolation

4.2.1 Electrocoagulation technique (EC)

The absorbance and electrolysis times of each sample solutions were shown in Table 4.1 and Fig. 4.1. The results showed the absorbance decrease when increase the time. After 30 min of the coagulation process seems to be almost unchanging and believed to be coagulated in EC process were chlorophyll and pigment.

Table 4.1 Absorbance of the sample solution after the electrocoagulation process

Time (min)	Absorbance of sample
0	3.0841
15	2.8122
30	2.5978
45	2.6151
60	2.5986
75	2.5207
90	2.3907
105	2.5325
120	2.4116

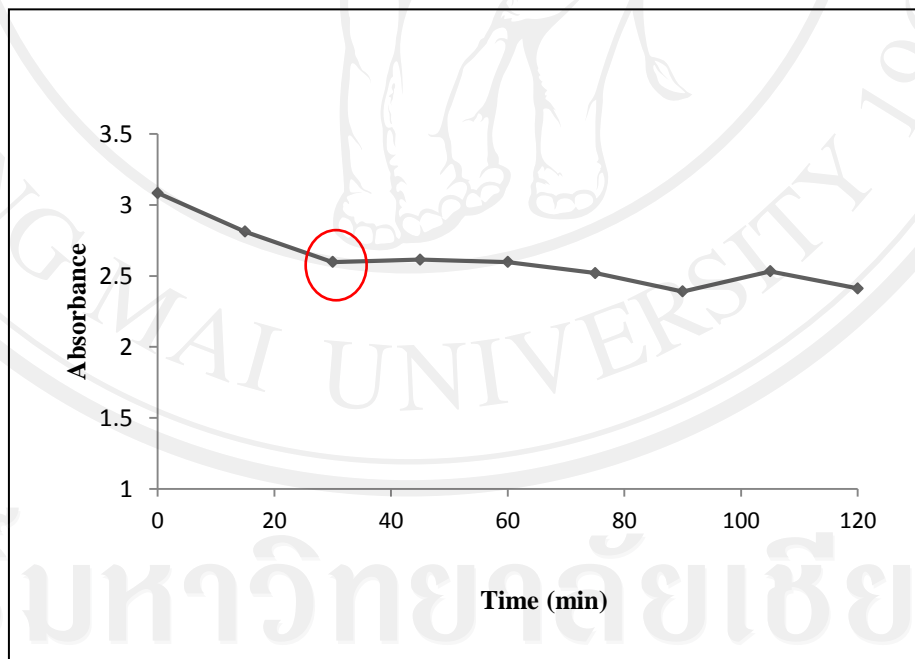


Figure 4.1 Plot of the absorbance and electrolysis time for the sample solution

at 242 nm

After EC process, the result showed the color of sample solution treated with EC process was lighter than sample solution from conventional technique (Fig. 4.2). This result could be explained that the most of chlorophyll was removed. The results of Thin Layer Chromatography (TLC) indicated that EC extract gave more similar components compared with conventional extract (Fig. 4.3).



Figure 4.2 The sample solution from conventional technique (a), after treated with EC process (b)

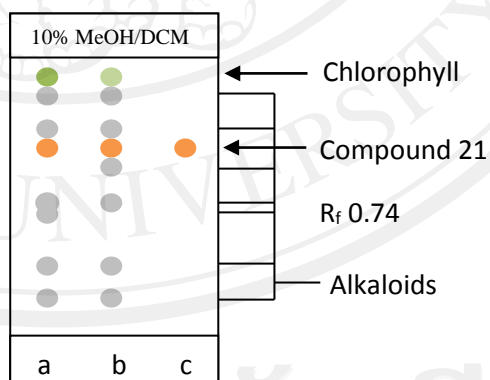
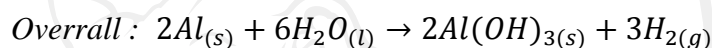
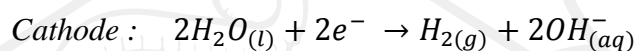


Figure 4.3 TLC of EC extract (a), conventional extract (b) and compound 21 (c) with 10 % MeOH:CH₂Cl₂

Chlorophyll and pigment would be coagulated because these coloring matters had some phenolic groups in their structure. The main reaction occurred during the electrolysis would normally produce aluminum ion (Al^{3+}) at the anode and hydroxide ion (OH^-) at the cathode. When aluminum ion bonded with hydroxide ion, aluminum hydroxide ($\text{Al}_3(\text{OH})_3$) were obtained look like gel. The reaction as shown below.



Chlorophyll was coagulated with $\text{Al}_3(\text{OH})_3$ by adsorption and then precipitates out of solution in the form of an insoluble salt. However, the aluminum ion at the anode may interact directly with phenol which precipitates out of the sample solution in form of an insoluble salt, e.g. aluminium triphenolate $[\text{Al}(\text{OAr})_3]$ ^[40] (Fig. 4.4).

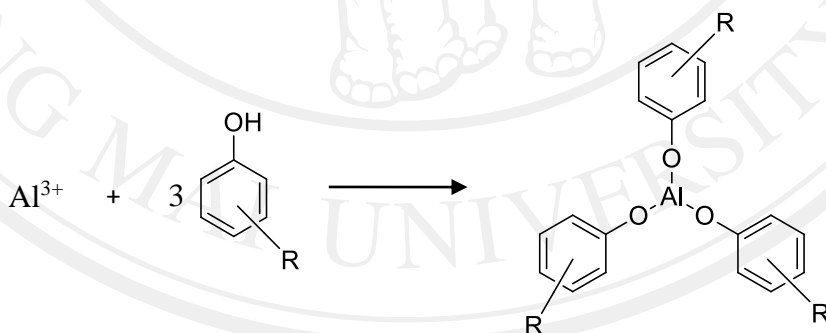


Figure 4.4 Electrocoagulation reaction type of phenolic compounds with Al^{3+} ^[40]

The reaction of electrocoagulation preferably coagulated with phenolic compounds (chlorophyll, tannins and pigments) which have adjacent (1,2-disubstitued or 1,2,3-trisubstitued) hydroxyl groups. However, the interaction of phenolic compounds with at least two adjacent hydroxyl groups seems to be more favorable

leading to preferential precipitation^[41]. Thus, the alkaloid with non-adjacent hydroxyl groups was almost unaffected by the EC process and still remain in the sample solution after 30 minutes of electrolysis times.

The ethanolic crude extract from EC process was partitioned with dichloromethane crude extract. This crude extract was isolated in two steps with quick column chromatography (QCC) using gradient elution with Hexane-CH₂Cl₂-MeOH (100:0:0 to 0:80:20) and finally isolated with column chromatography (CC) using gradient elution with Me₂CO-CH₂Cl₂ (20:80 to 100:0) to obtain compound 21 as shown in Fig. 3.3.

Other fractions that contained compound 21 were isolated by QCC and CC. The isolated compounds were compared with compound 21 on TLC plate at 254 nm and detected with Dragendroff's reagent to give orange spot as shown in Fig. 3.4–3.5. The mixture compounds i.e. fraction E22.9.4 and fraction E21*7 were isolated with reverse-phase high performance chromatography (RP-HPLC) to determine the quantity of compound 21.

4.2.2 Conventional technique (Solvent extraction)

The ethanolic extract was partitioned with dichloromethane to give dichloromethane extract. This material was isolated with QCC and CC as shown in Fig. 3.6 – 3.7 to give fraction F18* and F16*7. These fraction were isolated with RP-HPLC for determination of compound 21.

4.3 Determination of compound 21 by RP-HPLC

In this study, compound 21 was used as a standard. This compound was determined in fraction E22.9.4, E21*7, F18* and F16*7 using RP-HPLC that described in section 3.5.

Stock standard solutions ($100 \mu\text{g.mL}^{-1}$) were prepared by weighing 1.0 mg of compound 21 in a 10 mL volumetric flask. A series of each standard solution containing 10, 20, 30, 40 and $50 \mu\text{g.mL}^{-1}$ was prepared from stock standard by dilution of mobile phase [MeCN/Buffer pH 2.6 (30:70)]. The solutions were analyzed by RP-HPLC using the conditions as described in section 3.5. The retention time of mobile phase were 1.739-1.745 min and retention time of compound 21 were 2.293-2.300 min. Their chromatograms were shown in Fig. 4.5-4.10. The results were shown in Table 4.2. The calibration curve was plotted between peak area versus concentration were shown in Fig. 4.11.

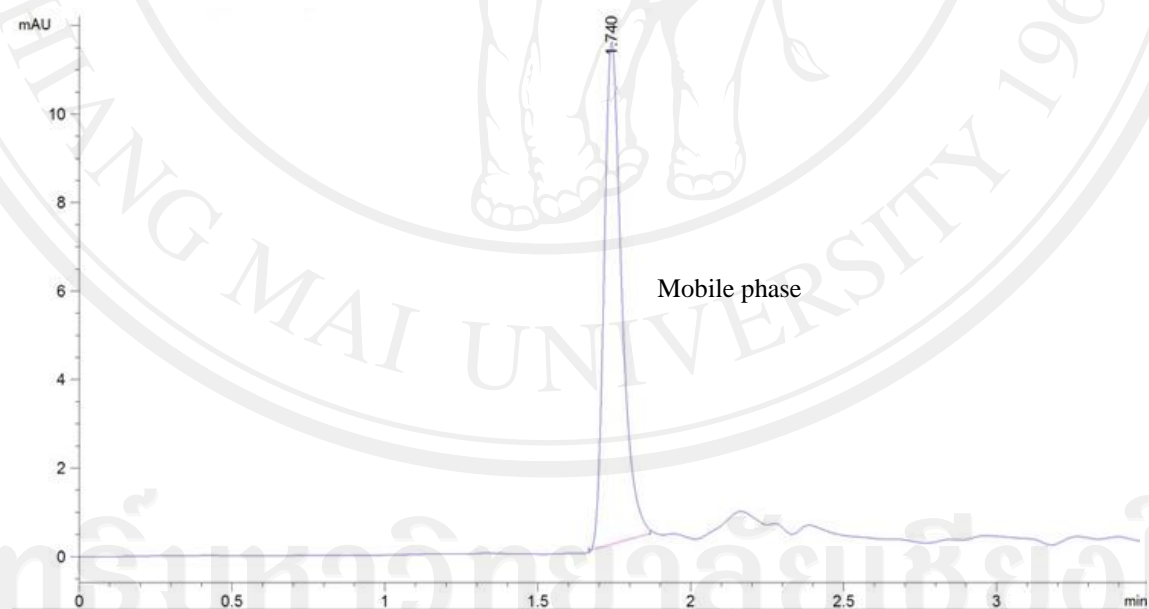


Figure 4.5 RP-HPLC chromatogram of mobile phase at 210 nm

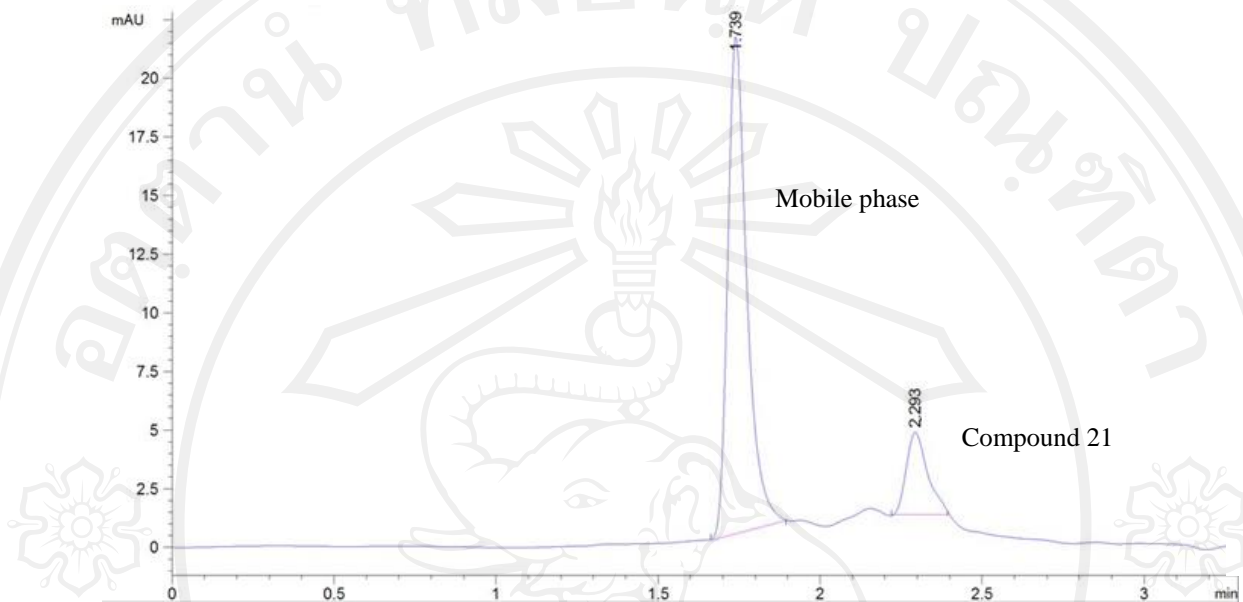


Figure 4.6 RP-HPLC chromatogram of 10 $\mu\text{g.mL}^{-1}$ standard solution

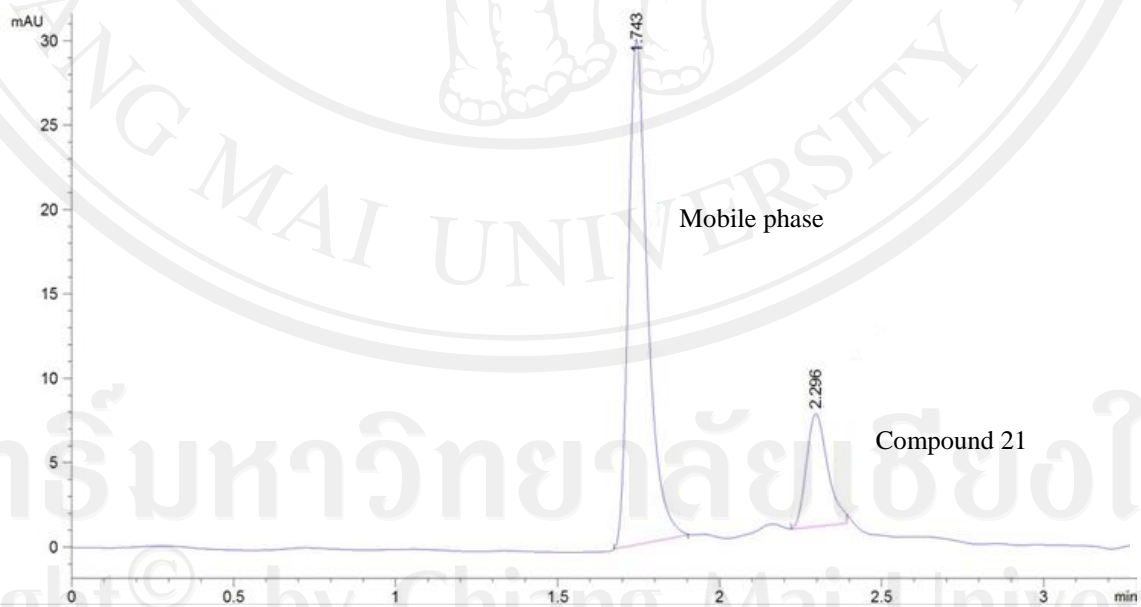


Figure 4.7 RP-HPLC chromatogram of 20 $\mu\text{g.mL}^{-1}$ standard solution

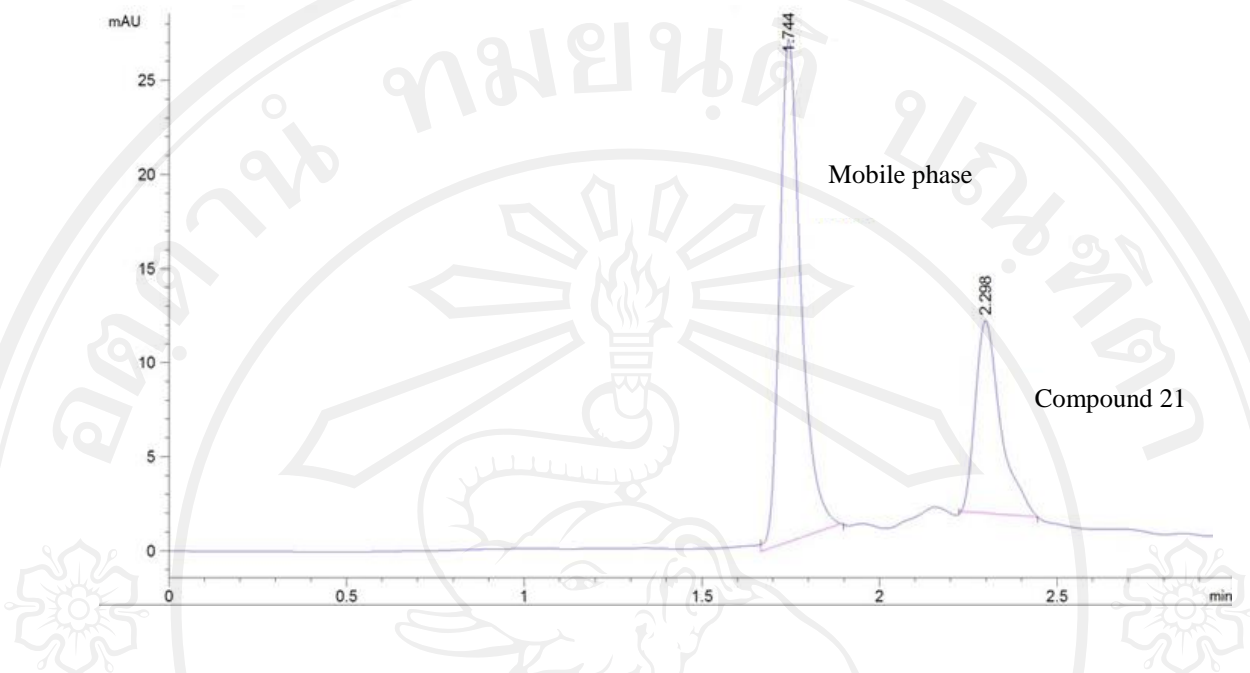


Figure 4.8 RP-HPLC chromatogram of $30 \mu\text{g.mL}^{-1}$ standard solution

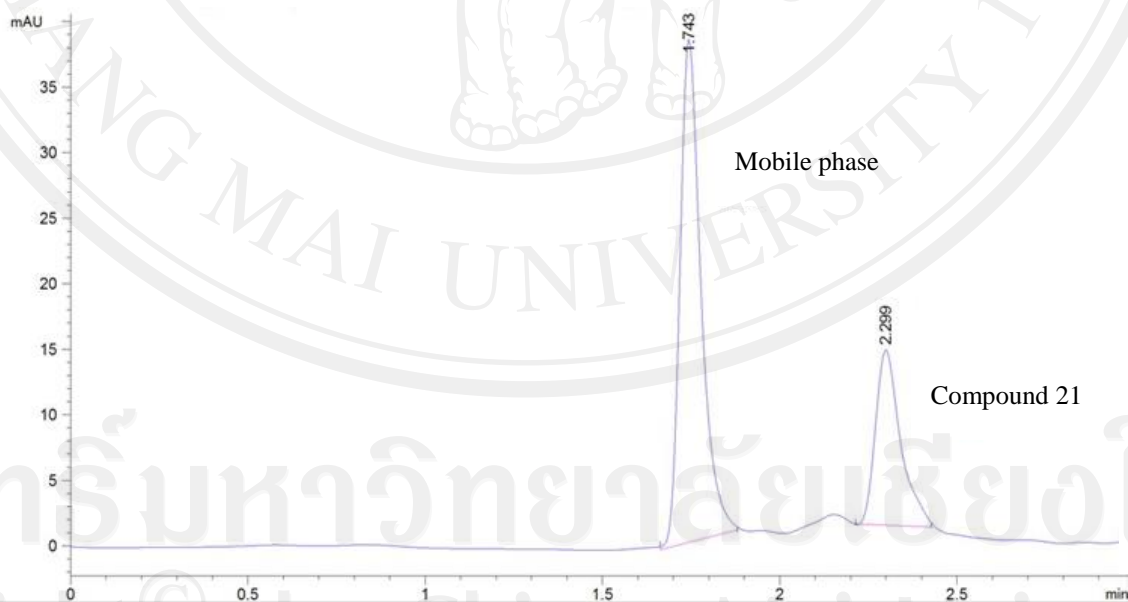


Figure 4.9 RP-HPLC chromatogram of $40 \mu\text{g.mL}^{-1}$ standard solution

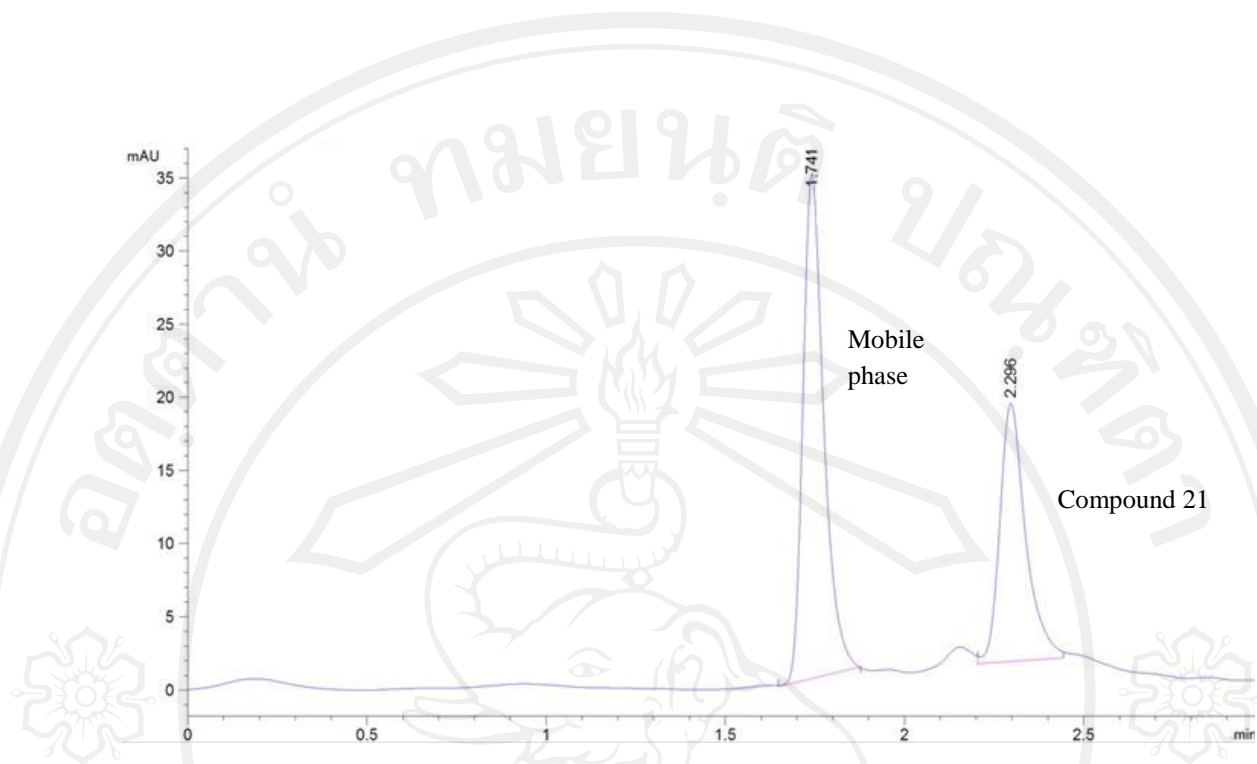


Figure 4.10 RP-HPLC chromatogram of $50 \mu\text{g.mL}^{-1}$ standard solution

Table 4.2 Calibration curve data of standard solutions (compound 21)

Sample	Retention time (min)		Area under curve (mAU)	Average area
	Mobile phase	Compound 21		
Mobile phase	1.740	-	-	-
Standard 10 $\mu\text{g.mL}^{-1}$	1.739	2.293	14.2542	13.5723
	1.745	2.299	13.1695	
	1.744	2.298	13.2933	
Standard 20 $\mu\text{g.mL}^{-1}$	1.743	2.296	31.1981	31.4384
	1.741	2.294	31.4602	
	1.742	2.295	31.6568	
Standard 30 $\mu\text{g.mL}^{-1}$	1.744	2.298	47.9715	48.0898
	1.741	2.295	48.1789	
	1.742	2.298	48.1190	
Standard 40 $\mu\text{g.mL}^{-1}$	1.743	2.299	65.0641	65.6032
	1.744	2.299	65.7489	
	1.742	2.297	65.9968	
Standard 50 $\mu\text{g.mL}^{-1}$	1.741	2.296	82.7962	83.2177
	1.743	2.300	83.6092	
	1.743	2.300	83.2477	

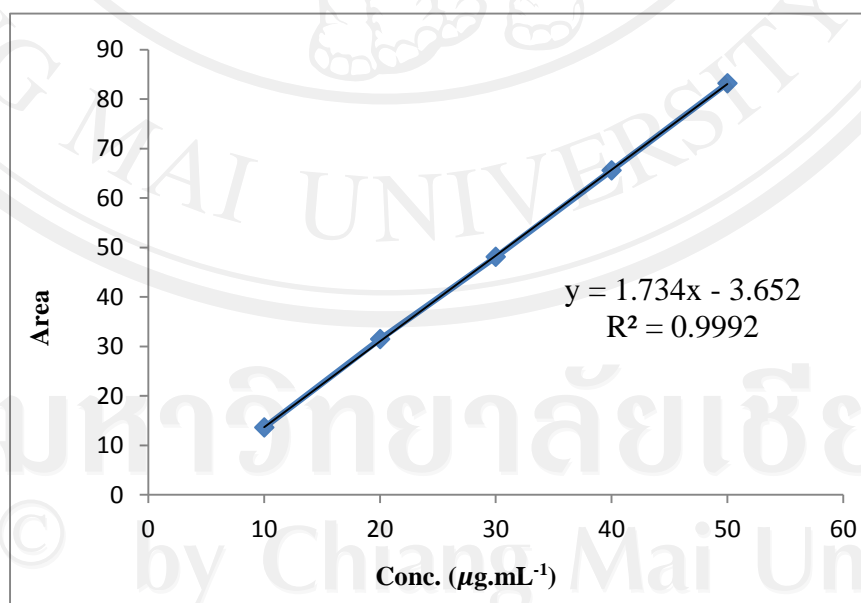


Figure 4.11 Calibration curve data of standard solution ranging from 10 to 50 $\mu\text{g.mL}^{-1}$

About 10 mg of each samples were accurately weighed 10.0 mg in a 10 mL volumetric flask and diluted by adding mobile phase [MeCN/Buffer pH 2.6 (30:70)] into $100 \mu\text{g}\cdot\text{mL}^{-1}$. The sample solutions were analyzed by RP-HPLC using the conditions as described in section 3.5. When injection of samples indicated that retention time of mobile phase were 1.735-1.742 min and retention time of compound 21 were 2.240-2.249 min. Their chromatograms were shown in Fig. 4.12-4.15. For determine, compound 21 of each sample was compared with calibration curve of standard solution. The results were shown in Table 4.3. The calculation of the sample were shown in appendix.

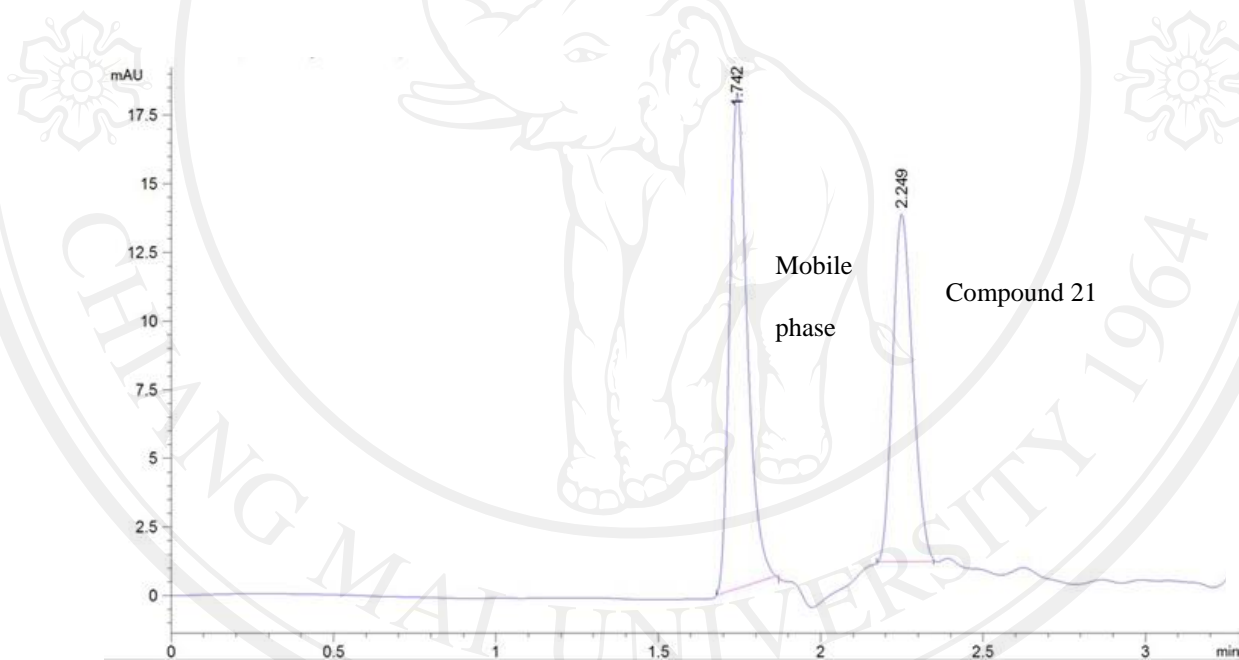


Figure 4.12 RP-HPLC chromatogram of fraction E22.9.4

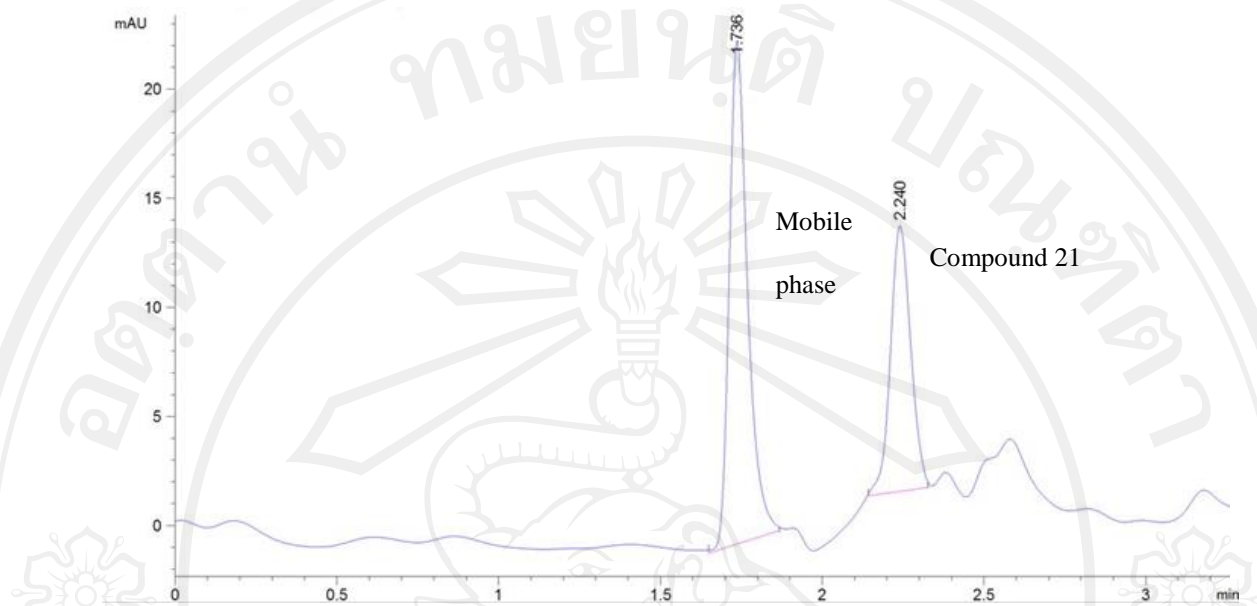


Figure 4.13 RP-HPLC chromatogram of fraction E21*7

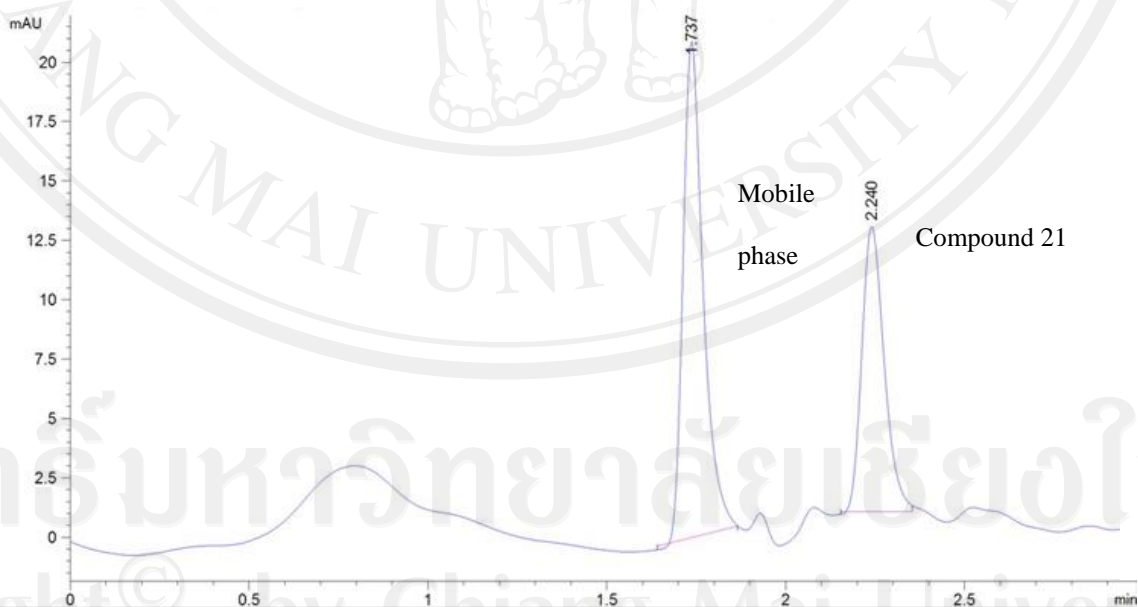


Figure 4.14 RP-HPLC chromatogram of fraction F16*7

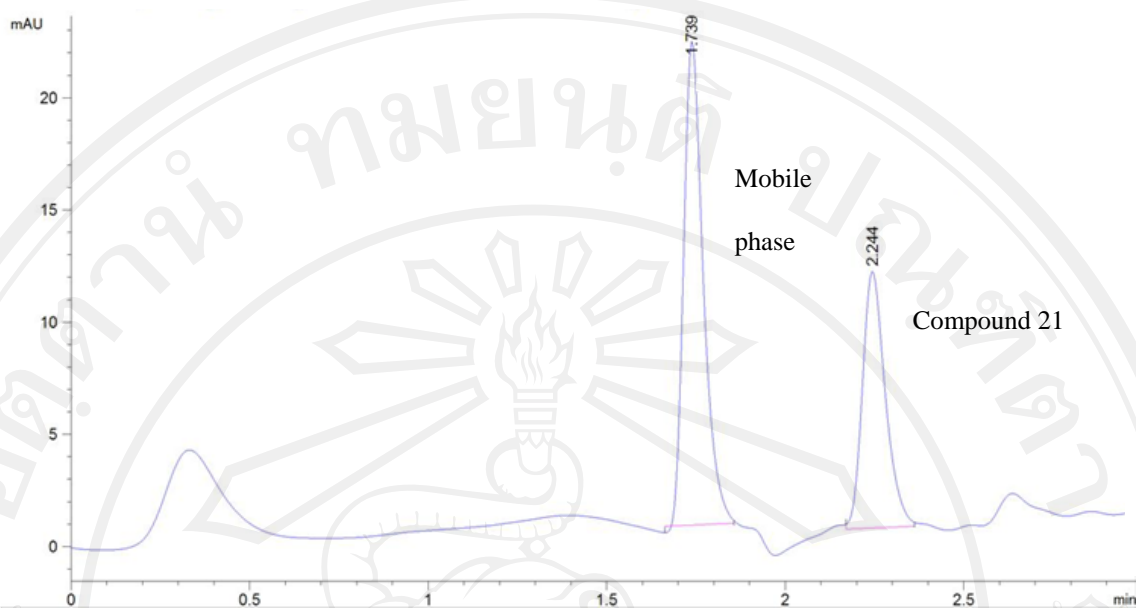


Figure 4.15 RP-HPLC chromatogram of fraction F18*

Table 4.3 RP-HPLC determination of compound 21 in the sample solutions

Sample	Retention time (min)		Area under Curve (mAU)	Average area	Conc. of Compound 21 ($\mu\text{g.mL}^{-1}$)	Sample weight (mg)	Compound 21 (mg)
	Mobile phase	Compound 21					
E22.9.4	1.742	2.249	54.7525	54.5958	33.5961	530.4	164.4
	1.736	2.243	54.8837				
	1.735	2.241	54.1512				
E21*7	1.736	2.240	50.2378	49.9959	30.9388	1,214	407.9
	1.741	2.246	49.0595				
	1.743	2.247	50.6904				
F16*7	1.737	2.240	50.9428	51.0134	31.5256	81.3	25.6
	1.739	2.243	50.7352				
	1.739	2.244	51.3621				
F18*	1.739	2.244	49.2388	49.2488	30.5080	1,708	520.9
	1.737	2.241	49.3273				
	1.735	2.238	49.1809				

Table 4.4 Quantitative of compound 21 by RP-HPLC determination

Technique	Weight of crude extract (g)	Fractions	Compound 21 (mg)	Percentage yield of compound 21 (%)
EC	70	E22.5	61.5	0.9
		E22.9.4	164.4	
		E21*7	407.9	
		Total	638.8	
Conventional	100	F16*7	25.6	0.5
		F18*	520.9	
		Total	546.5	

The results in Table 4.4 indicated that the percentage yield of compound 21 from EC technique (0.9%) is higher than conventional technique (0.5%).

4.4 Structure elucidation of compound 21

The structural elucidation of compound 21 was analysed by their spectroscopic data and comparison of spectral data with those published previously in literature^[42].

Compound 21 was obtained as a yellow-brown solid; HRMS 340.1549 [M+H]⁺ calcd. for C₂₀H₂₁NO₄ 340.1549 (Fig. 4.16). The aporphine chromophore was evident by UV (Fig. 4.17) absorption bands at λ_{max} 221, 227 and 314 nm. The FT-IR spectrum (Fig. 4.18) showed the absorption bands of CH stretching at 2953, 2911, 2842, 2826 cm⁻¹, CH stretching of aromatic at 1606, 1515, 1460 cm⁻¹, C-N stretching at 1390, 1341 cm⁻¹ and C-O stretching at 1096, 1048 cm⁻¹. The ¹H-NMR spectrum (Fig. 4.19 and Table 4.4) showed the sharp singlet signals of three aromatic protons at δ 7.65, 6.76 and 6.49, signals of four methylene protons at δ 6.06 (*s*, 1H) and 5.91 (*s*, 1H) which was the methylenedioxy protons, δ 3.17-3.02 (*m*, 3H) and 2.68-2.49 (*m*, 3H), the signals of two methoxy protons at δ 3.91 (*s*, 3H) and 3.90 (*s*, 3H), the signal of methine proton at δ 3.17-3.02 (*s*, 1H) and methyl proton at δ 2.54 (*s*, 3H) which connected to N atom. The ¹³C-NMR spectrum (Fig. 4.20 and Table 4.5) showed nine quarternary carbons at δ 148.2, 147.6, 146.6, 141.7, 128.2, 126.4, 126.1, 123.4 and 116.5, four methine carbons at δ 111.2, 110.4, 106.7 and 62.2, four methylene carbons at δ 53.4, 34.0 and 28.9, two methoxy carbons at δ 56.0 and 55.8, N-methyl carbon at δ 43.6, respectively. This compound was confirmed by the 2D NMR data (Fig. 4.22-4.24 and Table 4.5). The lowest field aromatic proton of aporphine core at δ 7.65 was assigned on C-11 (δ 110.4). The HMBC correlation of this proton correlated with C-1a (δ 116.5), C-7a (δ 128.2), C-9 (δ 148.2), C-10 (δ 147.6) and C-11a (δ 123.4). Two methoxy protons at δ 3.91 and 3.90 (each *s*, 3H), showed correlate at C-9 and C-10 which supported that substituted on

C-9 and C-10, respectively. The aromatic protons at δ 6.76 was located at C-8 (δ 111.2) by HMQC data which correlated with C-7 (δ 34.0), C-7a, C-9, C-10 and C-11a, respectively. The methylene protons (δ 3.17-3.02, 2.68-2.49) at C-7 gave cross peak with the methine proton (δ 3.17-3.02) at C-6a in COSY spectrum. The methylene protons was attributed at C-7 because of HMBC data of methylene proton (δ 3.17-3.02, 2.68-2.49) showed cross peak with C-1b (δ 126.1), C-6a (δ 62.2), C-7, C-8 and C-11a. Moreover, the highest field methyl group at δ 2.54 replaced on N-atom showed cross peaks with C-5 (δ 53.4) and C-6a by HMBC. Another cross peaks from COSY spectrum was two groups of methylene protons at δ 3.17-3.02(*m*) and 2.68-2.49(*m*) that were located at C-4 (δ 28.9) and C-5, respectively. The HMBC spectrum of methylene protons at C-4 showed cross peaks with C-1b (δ 126.1), C-3 (δ 106.7), C-3a (δ 126.4) and C-5. These results confirmed the position of two methylene groups. The HMBC correlation of the last aromatic proton at δ 6.49 indicated that this proton was located at C-3. In addition, the methylenedioxy protons at δ 6.06 and 5.91 was attached to C-1 (δ 141.7) and C-2 (δ 141.6) positions of aporphine skeleton by HMBC data caused cross peaks with C-1 and C-2.

The structure of compound 21 was confirmed to be dicentrine, a known alkaloid^[42], by 1D and 2D NMR data.

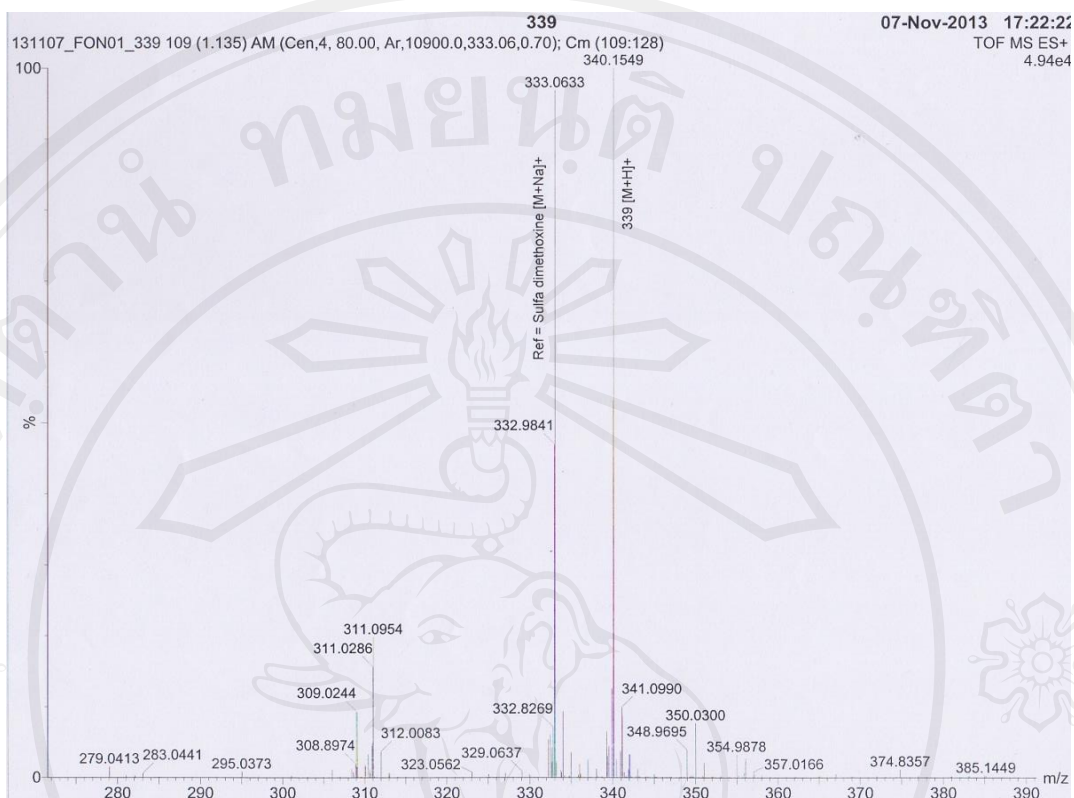


Figure 4.16 Mass spectrum of compound 21

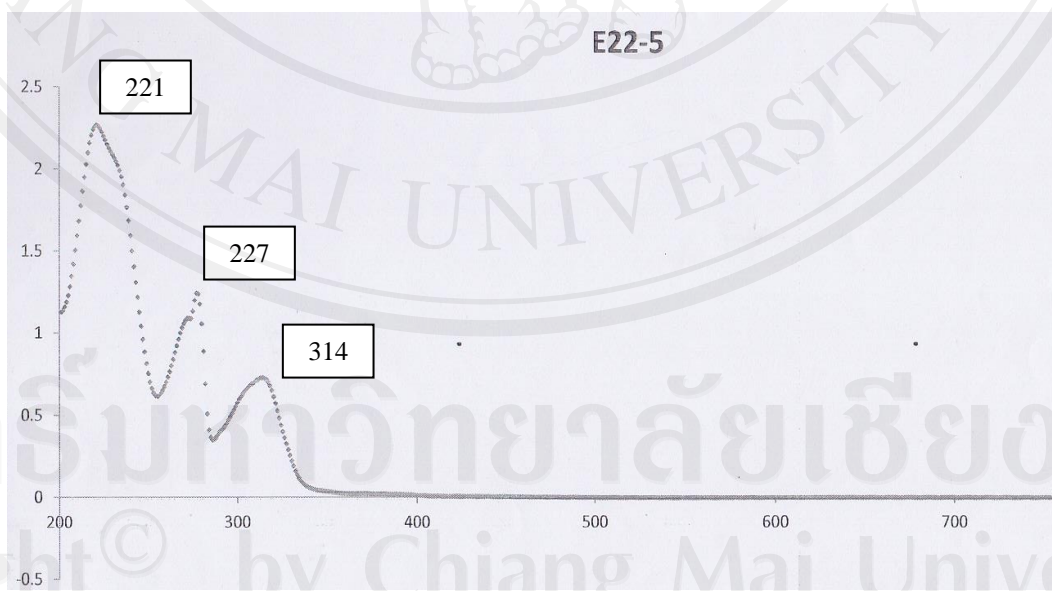


Figure 4.17 UV (MeOH) spectrum of compound 21

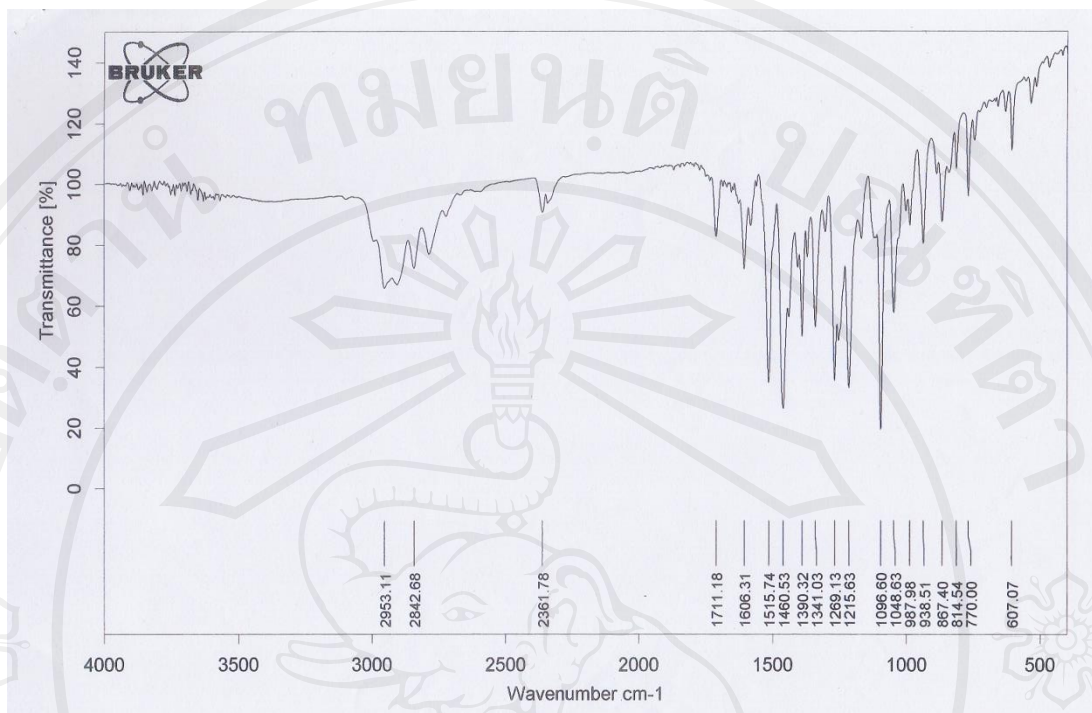


Figure 4.18 FTIR (neat) spectrum of compound 21

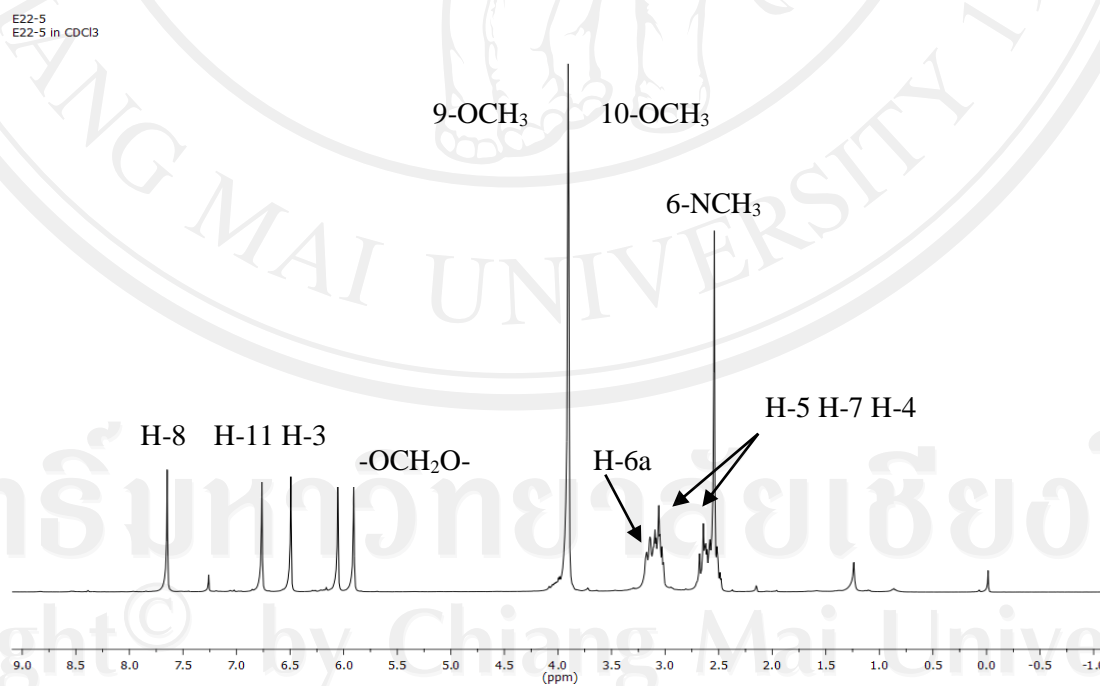


Figure 4.19 ¹H-NMR spectrum 400 MHz (CDCl₃) of compound 21

E22-5
E22-5 in CDCl₃---13C

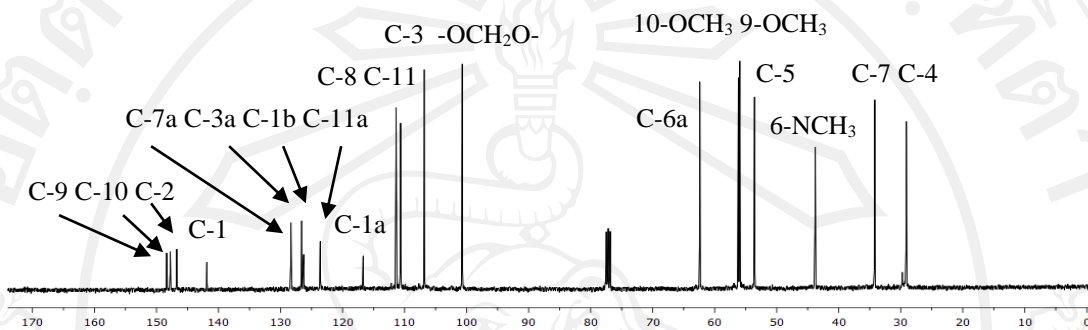
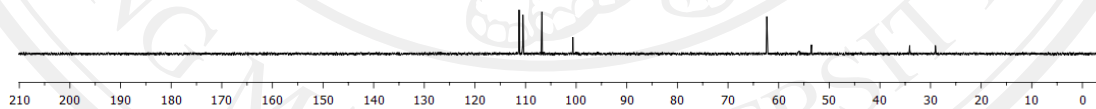


Figure 4.20 ¹³C-NMR spectrum 100 MHz (CDCl₃) of compound 21

E22-5
E22-5 in CDCl₃---DEPT 90



E22-5
E22-5 in CDCl₃---DEPT 135

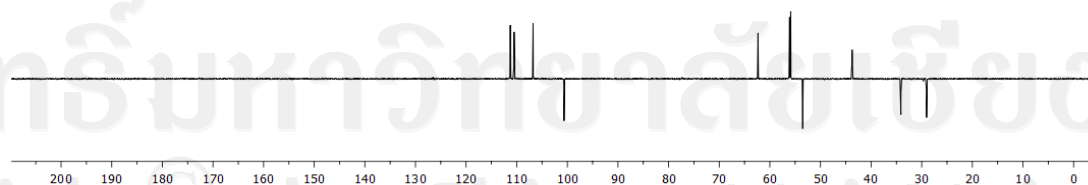


Figure 4.21 DEPT spectrum of compound 21

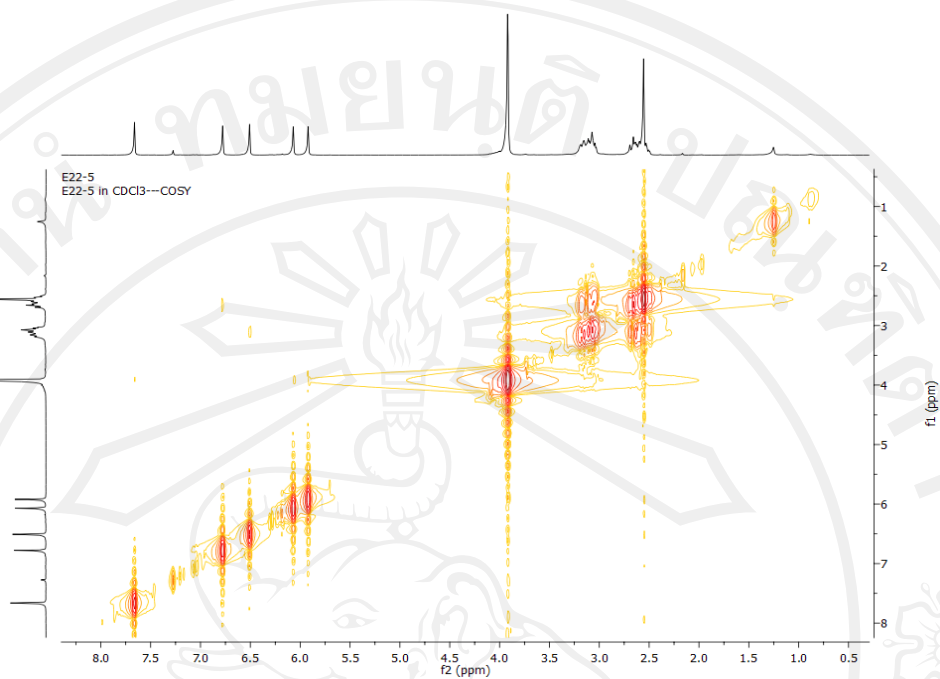


Figure 4.22 2D COSY spectrum of compound 21

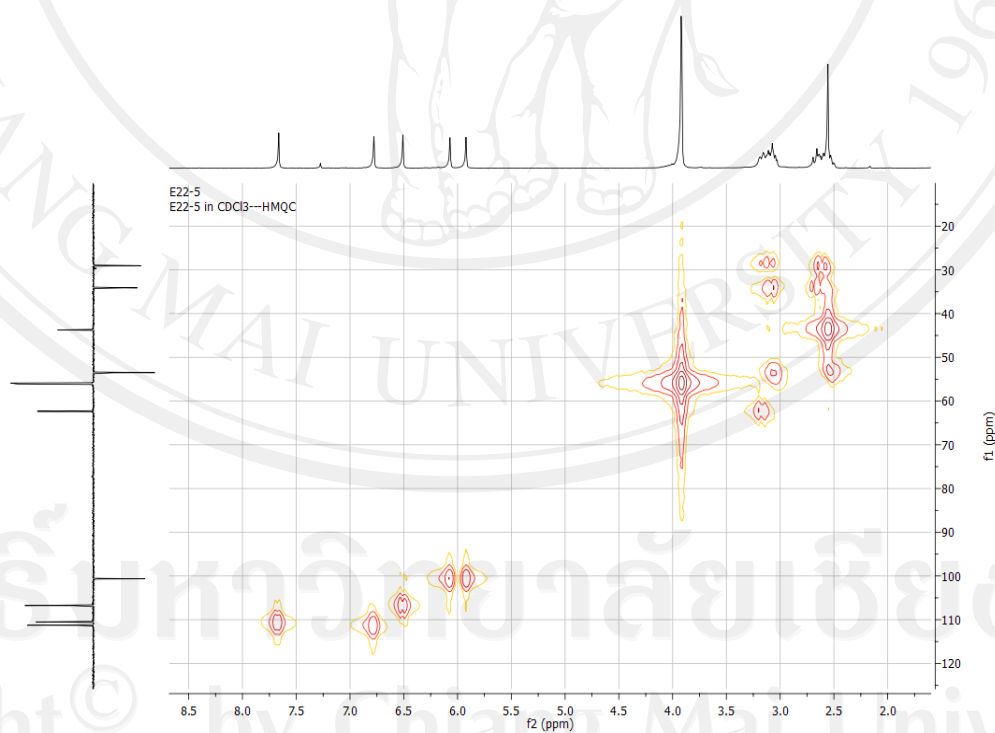


Figure 4.23 2D HMQC spectrum of compound 21

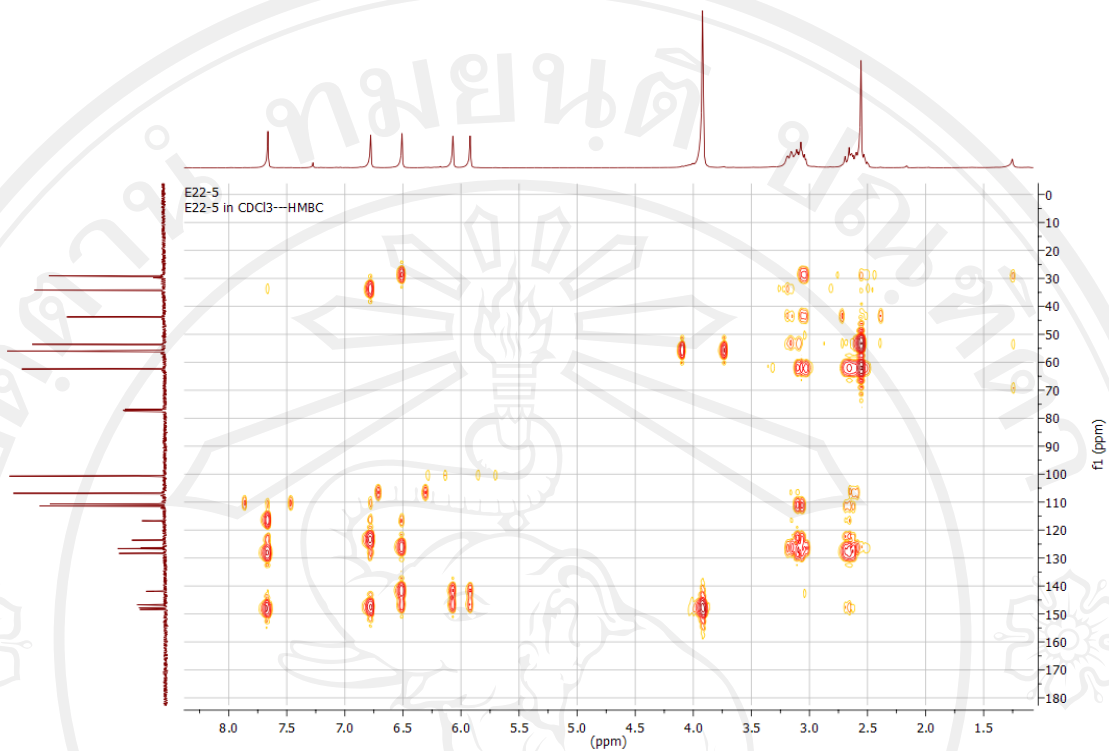


Figure 4.24 2D HMBC spectrum of compound 21

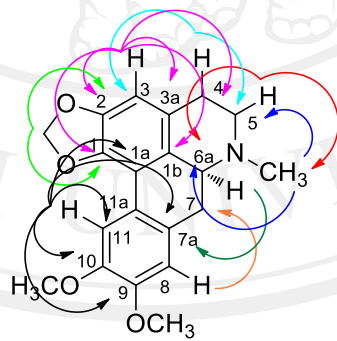


Figure 4.25 The HMBC correlation of dicentrine (compound 21)

Table 4.5 $^1\text{H-NMR}$ (400 MHz), $^{13}\text{C-NMR}$ (100 MHz) and HMBC correlation of

compound 21

Data	$^1\text{H-NMR}$ (400 MHz, CDCl_3)	$^{13}\text{C-NMR}$ (100 MHz, CDCl_3)	HMBC correlation
Position	δ_{H} (mult., J (Hz))	δ_{C} (mult., J (Hz))	
9	-	148.2	-
10	-	147.6	-
2	-	146.6	-
1	-	141.7	-
7a	-	128.2	-
3a	-	126.4	-
1b	-	126.1	-
11a	-	123.4	-
1a	-	116.5	-
8	6.76 (s, 1H)	111.3	C-7, C-7a, C-9, C-10, C-11a
11	7.65 (s, 1H)	110.4	C-1a, C-7a, C-9, C-10, C-11a
3	6.49 (s, 1H)	106.7	C-1, C-1b, C-2, C-3a, C-4
-OCH ₂ O-	6.06 (s, 1H)	100.5	C-1, C-2
	5.91 (s, 1H)		C-1, C-2
6a	3.17-3.02 (m, 1H)	62.2	C-1b, C-3a, 6-NCH ₃ , C-7
10-OCH ₃	3.90 (s, 3H)	56.0	C-10
9-OCH ₃	3.91 (s, 3H)	55.8	C-9
5	3.17-3.02 (m, 1H)	53.4	C-4, C-6a, 6-NCH ₃
	2.68-2.49 (m, 1H)		C-3a, C-4, C-6a
6-NCH ₃	2.54 (s, 3H)	43.6	C-5, C-6a
7	3.17-3.02 (m, 1H)	34.0	C-6a, C-7, C-8, C-11a
	2.68-2.49 (m, 1H)		C-1b, C-6a, C-8, C-11a
4	3.17-3.02 (m, 1H)	28.9	C-1b, C-3a, C-5
	2.68-2.49 (m, 1H)		C-1b, C-3, C-3a

4.5 Determination of efficiency on acetylcholinesterase inhibitory activity by TLC

bioautographic assay

A study of the acetylcholinesterase (AChE) inhibitory activity of conventional extract, EC extract and dicentrine (compound 21) were performed by TLC bioautographic assay. The AChE inhibition appeared as white spots on a purple background of the chromatogram (Fig. 4.26). Galantamine was used as a positive control and MeOH was used as a negative control. The results showed in Table 4.6.

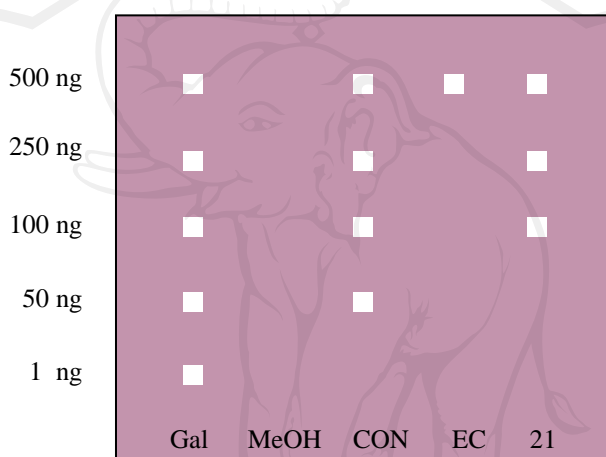


Figure 4.26 Bioautographic thin layer chromatography showing the acetylcholinesterase inhibition of all samples and standard (galantamine). Gal=galantamine, MeOH=methanol, Con=conventional extract, EC=EC extract and 21=dicentrine

Table 4.6 The minimum AChE inhibitory concentrations of samples required to inhibit

AChE	Samples	Minimum inhibitory requirement (ng)
	Conventional extract	50
	EC extract	500
	Dicentrine	100
	Galantamine (positive control)	1
	MeOH (negative control)	-

4.6 Biological Activity test

The toxicity of conventional extract, EC extract and dicentrine were elucidated by brine shrimp lethality activity test. $K_2Cr_2O_7$ was used as a positive control and DMSO was used as a negative control. The results shown in Table 4.7-4.10.

Table 4.7 The LC_{50} values of samples from *D. obtusipetalum* against brine shrimp (*Artemia salina* Leach)

Samples	$LC_{50} \pm S.D. (\mu g.mL^{-1})$
Conventional extract	24.646 \pm 0.227
EC extract	33.124 \pm 0.217
Dicentrine	56.69 \pm 0.360
$K_2Cr_2O_7$ (positive control)	16.52 \pm 0.194
DMSO (negative control)	-

Table 4.8 Mortality of the brine shrimp larvae after 24 hr of exposure to various concentration of conventional extract

Dose ($\mu\text{g/mL}$)	Dosage (log dose)	Dead	Alive	Accumulated alive	Accumulated dead	Ratio Dead: Total	Mortality (%)
160	2.204	30	0	0	103	30:30	100
80	1.903	28	2	2	73	28:30	93
40	1.602	25	5	12	45	25:30	83
20	1.301	13	17	27	20	13:30	43
10	1.000	7	13	49	7	7:30	23

Estimated $LC_{50} = 24.646 \pm 0.227 \mu\text{g.mL}^{-1}$

Table 4.9 Mortality of the brine shrimp larvae after 24 hr of exposure to various concentration of EC extract

Dose ($\mu\text{g/mL}$)	Dosage (log dose)	Dead	Alive	Accumulated alive	Accumulated dead	Ratio Dead: Total	Mortality (%)
160	2.204	30	0	0	93	30:30	100
80	1.903	27	3	3	63	27:30	90
40	1.602	18	12	15	36	18:30	60
20	1.301	12	18	33	18	12:30	40
10	1.000	6	24	57	6	6:30	20

Estimated $LC_{50} = 33.124 \pm 0.217 \mu\text{g.mL}^{-1}$

Table 4.10 Mortality of the brine shrimp larvae after 24 hr of exposure to various concentration of dicentrine

Dose ($\mu\text{g/mL}$)	Dosage (log dose)	Dead	Alive	Accumulated alive	Accumulated dead	Ratio Dead: Total	Mortality (%)
160	2.204	30	0	0	64	30:30	100
80	1.903	26	4	4	34	26:30	87
40	1.602	6	24	28	8	6:30	20
20	1.301	2	28	56	2	2:30	6.7
10	1.000	0	30	86	0	0:30	-

Estimated $LC_{50} = 56.69 \pm 0.360 \mu\text{g.mL}^{-1}$

The results from Table 4.6 and Table 4.7 showed the conventional extract was the most effective AChE inhibitor with minimum inhibitory requirement (MIR) of 50 ng and had the highest activity against brine shrimp with LC_{50} value of $24.646 \pm 0.227 \mu\text{g.mL}^{-1}$. The reason could be explained that the conventional extract contain many components which have AChE inhibitory activity and brine shrimp toxicity. On the other hand the active compounds in EC extract may be decomposed due to the high temperature from EC process. EC extract and dicentrine were able to inhibit AChE with MIR of 500 and 100 ng, respectively and had activity against brine shrimp with LC_{50} value of 33.124 ± 0.217 and $56.69 \pm 0.360 \mu\text{g.mL}^{-1}$, respectively.

Moreover, cytotoxic, anti-cancer, anti-malarial and anti-mycrobacterium activities of dicentrine were evaluated by National Center for Genetic Engineering and Biotechnology (BIOTEC). The results were shown in Table 4.11.

Table 4.11 Biological activities of dicentrine from *D. obtusifolium*

Biological activities test		Positive control	Dicentrine
Cytotoxicity (IC ₅₀ , µg/mL)	vero cells (American green monkey kidney)	0.692 ^a	2.72
Anti-cancer (IC ₅₀ , µg/mL)	oral cavity cancer (KB)	1.21 ^a , 1.12 ^b	8.66
	small lung cancer (NCI-H187)	0.935 ^a , 0.139 ^b	4.36
	breast cancer (MCF-7)	7.90 ^b , 7.00 ^c	8.42
Anti-malarial (<i>Plasmodium falciparum</i>) (IC ₅₀ , µg/mL)		1.91 ^d , 0.0247 ^e	0.32
Anti-mycobacterium (Anti-TB) (MIC, µg/mL)		0.025 ^f , 0.047 ^g , 1.88 ^h , 0.625 ⁱ , 0.781 ^j	50

Cytotoxic assay :

- a = Ellipticine
- b = Doxorubicin
- c = Tamoxifen
- d = Dihydroartemisinin
- e = Mefloquine
- f = Rifampicin
- g = Isoniazid
- h = Ethambutal
- i = Streptomycin
- j = Ofloxacin

The results showed dicentrine had cytotoxicity activity against vero cells (American green monkey kidney) with IC₅₀ value of 2.72 µg.mL⁻¹, anticancer activity against oral cavity cancer (KB), small lung cancer (NCI-H187) and breast cancer (MCF-7) with IC₅₀ value of 8.66, 4.36 and 8.42 µg.mL⁻¹, respectively. As well as,

triterpenoids and flavanone from *D. dasymaschalum* exhibited potent cytotoxicity activity against human lung cancer cell lines (NCI-H187)^[7]. Moreover, dicentrine showed antimalarial activity with IC₅₀ value of 0.32 µg.mL⁻¹ and mycobacterium (anti-TB) activity with minimum inhibitory concentration (MIC) value of 50 µg.mL⁻¹.

A comparison of the anti-breast cancer (MCF-7) activity between dicentrine and doxorubicin (positive control) indicated that dicentrine had similar effective with positive control. This result suggested that this compound is unsuitable for using as anti-breast cancer drug because it can destroy normal cells in human.